Materials Chemistry Horizons RESEARCH

Adsorption of Methyl Orange onto Biosorbent from Pistachio Shell: Effects of Different Activation Methods

Hadi Baseri [a,*], Pooya Fazlali [b], Amir Hussein Hooshmand Poor [a]

[a] School of Chemistry, Damghan University, Damghan, Iran.
[b] Technical University of Berlin and university of Potsdam, Berlin, Germany.

***Corresponding author**: baseri@du.ac.ir (H. Baseri)

Mater. Chem. Horizons, 2025, 4(1), 49-58 10.22128/mch.2026.3083.1070 OPEN ACCESS

ABSTRACT

Agricultural waste represents a significant source of various bio-products that can help mitigate environmental pollution and greenhouse gas emissions, while also reducing our reliance on fossil resources. This study focuses on the production of high-value biosorbents derived from pistachio hard skin (PHS). The biomass of PHS was utilized as a precursor for the development of different biosorbents through three distinct activation methods: solvent extraction, chemical activation with phosphoric acid, and pyrolysis processes. The produced biosorbents were characterized using X-ray diffraction (XRD), Fourier-transform infrared spectroscopy (FTIR), scanning electron microscopy (SEM), and energy-dispersive X-ray spectroscopy (EDS) analyses. Depending on the activation methods employed, the adsorption capacities of the biosorbents for the Methyl Orange (MO) dye component varied from approximately 100 to 700 mg/g. Notably, the maximum adsorption capacity was achieved after the pyrolysis process. Furthermore, isotherm studies indicated that the Sips and Langmuir isotherm models provided a relatively better fit for the experimental data, with R^2 values of 0.999 and 0.983, respectively.

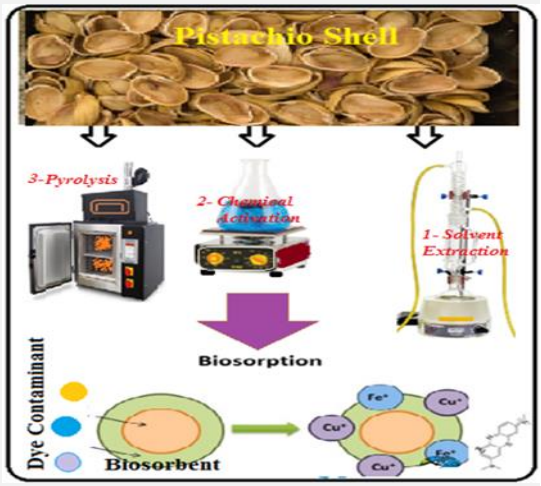

Keywords: Biosorbent, pistachio hard skin, methyl orange, biomass

1. Introduction

Plant waste refers to the organic materials discarded during agricultural and industrial processes, including leaves, stems, roots, and other by-products. It is estimated that approximately 1.3 billion tons of plant waste are generated annually worldwide. This total encompasses waste from crops, forestry, and food processing [1, 2, 3].

The largest contributors to plant waste are agriculture (particularly from cereal crops), horticulture, and the food processing industries. A significant portion of this waste ends up in landfills, contributing to methane emissions, a potent greenhouse gas [4,5]. However, agricultural wastes also have various important applications across different industries. For instance: Plant waste can be converted into bioenergy through processes such as anaerobic digestion or combustion, providing a renewable energy source [6]. Composting plant waste enriches the soil, improves soil structure, and promotes healthy plant growth by returning essential nutrients to the earth [7]. Certain plant wastes contain compounds that can be extracted for use in pharmaceuticals and nutraceuticals [8].

Given the rapid growth of industries in recent years and the large volume of wastewater produced, the use of various wastewater treatment processes has garnered significant attention from researchers [9]. The adsorption of different pollutants using adsorbents made from organic and inorganic materials [10] is one of the essential processes for removing contaminants and treating industrial and domestic wastewater. In this context, various adsorbents have been developed by researchers and utilized for the removal of different colored substances from contaminated water. These adsorbents are derived from a variety of precursors, including different types of organic polymers, mineral materials, agricultural waste, and others [11, 12]. The production of various biosorbents from different plant wastes for the removal of various contaminants has been reported in the literature [13-18]. For example, the adsorption

Received: October 03, 2025
Received in revised: November 02, 2025
Accepted: December 20, 2025

performance of Pinus brutia cone powder was demonstrated for the removal of Basic Fuchsin dye from aqueous solutions [13]. The used raw materials were modified through calcination and chemical activation with phosphoric acid, reporting a maximum dye removal efficiency exceeding 95% under acidic conditions.

Cinnamon bark waste was utilized for the adsorption of Pb^{2+}, Cd^{2+}, and Cu^{2+} ions from contaminated water, achieving adsorption capacities of 12.3, 3.1, and 2.22 mg/g, respectively. The best-fitted isotherm for the adsorption of Pb^{2+} by the cinnamon bark waste was the Langmuir model, while the Freundlich model was more suitable for Cd^{2+} and Cu^{2+} ions [14]. The production of cost-effective adsorbents with high adsorption efficiency for pollutants is a crucial option in the treatment of industrial wastewater. Utilizing agricultural and food waste as precursors for these adsorbents can significantly reduce production costs. However, adsorbents derived from plant waste typically exhibit low adsorption efficiency. To improve this low adsorption performance, activation using various methods is necessary. Nonetheless, these activation processes can increase the overall cost of the adsorbents. Therefore, it is essential to evaluate the impact of different activation processes on adsorption efficiency and to compare the adsorbents produced through various activation methods.

In this study, the biomass of pistachio hard skin (PHS) was employed as the precursor for biosorbent production and it was used for the adsorption of a model dye contaminant of Methyl Orange from contaminated water. Additionally, the effects of various physical and chemical activation methods on the adsorption capacity of the produced biosorbent were examined and the produced biosorbents with different activation methods were compared.

2. Expriemnetal

2.1. Materials and measurements

The pistachio hard skin (PHS) was sourced from farms in Damghan (Semnan, Iran) from 10 to 15-year-old trees. The raw PHS, with a moisture content of approximately 10%, was dried in an oven at 100°C for 10 h, reducing the moisture content to below 3%. Subsequently, it was crushed and ground using a knife grinder to achieve particle sizes of less than 2 mm. Phosphoric acid, with a purity of approximately 85%, was purchased from Sigma-Aldrich. Ethanol (96%) was obtained from Ghatran Shimi (Iran), and nitrogen gas, with a purity exceeding 99.5%, was sourced from Sabalan Co. (Iran).

Fourier Transform Infrared (FTIR) spectroscopy with a Unicam 4600 FTIR spectrometer (Mattson, USA) was used for studding the organic structures and functional groups in the different produced biosorbents with scanning wave numbers from 400 to 4000 cm^{-1}. The morphology and shape of the particles on the surface of the produced biosorbents were examined using a Field-Emission Scanning Electron Microscope (FE-SEM) (TESCAN BRNO-MIRA3 LUM). The crystalline phases of the synthesized biosorbents were determined by X-ray diffraction analyses (XRD) with a D8-advanced instrument (BRUKER AXS, Karlsruhe, Germany) using Cu-Kα X-ray as a radiation source, (wavelength λ = 1.541874 ˚A) in a 2θ range of 5°–70°. The gravimetric method has been used to determine the moisture content of samples in which the sample weighed prior to and after drying in an oven at 120°C for 24 h.

2.2. Production of biosorbent

Soxhlet extraction was employed to separate the extractable components from the raw PHS. In this process, a 15 g sample of PHS powder was placed in a thimble, and extraction was conducted using 250 mL of 96% ethanol in a Soxhlet extractor (ASEMANLAB, Iran) for 24 h. After the extraction process, the remaining sawdust was dried in an oven at 80 °C for 12 h. In chemical activation process, for relatively better characteristics of the produced biosorbent, the impregnation ration of 2.5 was selected [19, 20], in which, about 10 g of the remaining powder from the extraction was mixed with a 100 ml phosphoric acid solution (H_3PO_4, 25% w/v) at 30 °C for 24 h in an Erlenmeyer flask under magnetic agitation. The powder was then separated by filtration and neutralized by washing with distilled water. Finally, it was dehydrated in an oven at 105 °C for 10 h. The final step in the production of the biosorbent is pyrolysis. In this process, an electrical furnace (8 cm inner diameter, 15 cm length, 500 W, and heating rate of about 50 °C/min) capable of reaching temperatures up to 700 °C (±5 °C) was used in fixed bed mode. Approximately 30 g of feedstock were charged into the furnace in a closed system, with a constant nitrogen flow rate of 3 cm^3/s and maintained at a constant temperature of 500 °C for 2 h. After the reaction, the system was allowed to cool for 3 h. Subsequently, the

nitrogen gas flow was cut off, the furnace was opened, and the residual biochar was collected in a closed vessel. The percents of weight reduction after solvent extraction, chemical activation, and pyrolysis are about 6%, 0%, and 70%.

2.3. Adsorption experiments

For the batch adsorption experiments, approximately 0.01 g of the biosorbent was added to 200 mL of the stock solution at the desired concentration. The system was mixed at 200 rpm using a heater stirrer for 1 hour at a constant temperature of 25°C. At the end of the experiment, the system was separated by filtration through filter paper, and the concentration of the remaining solution was determined using a UV/Vis spectrophotometer. The adsorption capacities q_t (mg/g) of the biosorbents were calculated using the following equation [21]:

$$q_t = \left(\frac{(C_i - C_f)}{m}\right) \times \mathrm{V} \quad (1)$$

In this equation, C_i and C_f are the initial and final concentrations of dye component (mg/L) in the reminded solution, m is the mass of used biosorbent (g), and V is the volume of solution (L). In this work, the effect of pH variations on the adsorption efficiency of the synthesized adsorbents was not investigated, and no substances were used to control the pH of the system. However, during the adsorption experiments, the pH of the system was measured, which ranged from 6 to 7.

3. Results and discussion

3.1. SEM analysis

The SEM images of the produced biosorbents after solvent extraction, phosphoric acid chemical activation, and pyrolysis are depicted in **Figure 1**. As shown, the produced biosorbent is a porous material with pores on its surface ranging in size from 500 nm to 20 µm. Moreover, the EDS analysis indicates the presence of carbon (C), oxygen (O), phosphorus (P), and silicon (Si) elements on the surface of the particles.

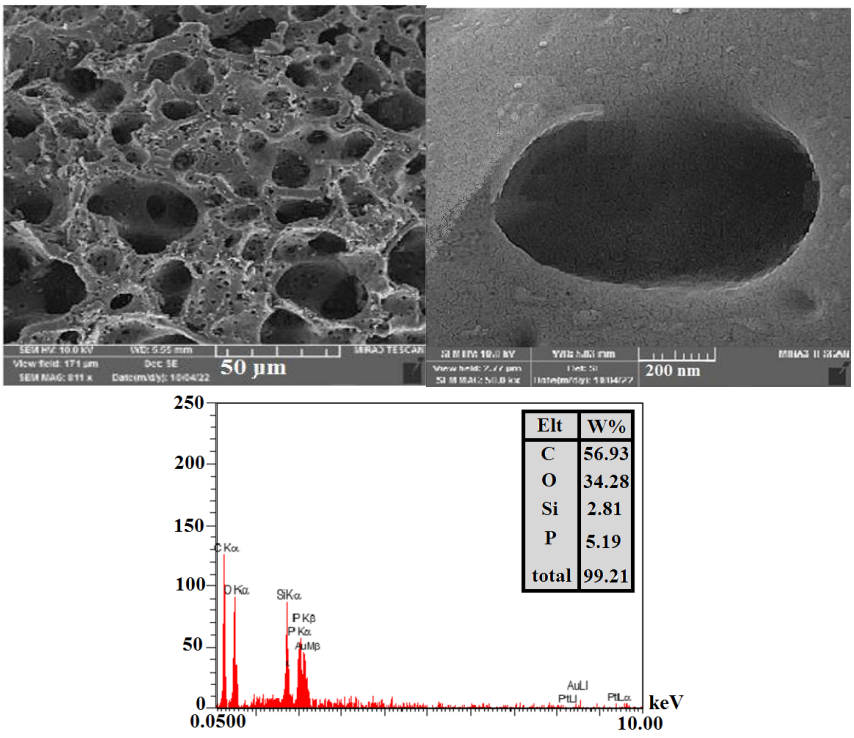

Figure 1. SEM images and EDS analysis of the produced biosorbent by chemical activation of PHS and pyrolyzed in 500 °C.

3.2. FTIR analysis

Figure 2 shows the FTIR spectra of PHS before and after solvent extraction, and after pyrolysis process. As expected, all the samples are primarily composed of lignin, cellulose, and hemicellulose which were exhibited the following main characteristic peaks: The broad band at approximately 3600 cm^{-1} is associated with hydroxyl groups (OH) in the cellulose structure as well as N-H bonds in amines [22, 23]. Furthermore, the bands in about 3000 cm^{-1} correspond to C-H bonds of methyl and methylene groups in hydrocarbons [24]. The bands in the range of 2400 to 2500 cm^{-1} are attributed to C=O bonds in carbonyls, carbon dioxide and so on. Moreover, C=O, O-C-O, and C=C of carbonyl, ether, and aromatic groups in hemicellulose and lignins are likely responsible for the peaks observed at approximately 1200 cm^{-1} [25, 26], the peaks around 1700 cm^{-1} may be related to C=C skeletal bands in aromatics or the stretching or bending of C=C groups in lignins [25]. Finally, the bands at 700 cm^{-1} are attributed to Si-O-Si bending vibrations or carbon halides [24]. Based on the results reported in **Figure 2**, after the pyrolysis process the concentration of O-H groups decreased significantly for all the studied samples. This reduction may be attributed to the significant decrease in water, alcohols, phenols, and other O-H containing components during the pyrolysis process. The vibration peaks at approximately 2400 cm^{-1} is attributed to C=O bonds in CO_2 molecules or carbonyls. The intensity of these peaks increased significantly after the pyrolysis process. The essential oils and the main parts of extractable components may be removed during extraction and pyrolysis processes, therefore the adsorption capacity of the samples increased. With the enhanced adsorption capacity of biosorbents, CO_2 molecules may be adsorbed more effectively on the surface of the particles and lead to higher intensity of the related peaks. The functional groups present on the surface of produced biosorbent can significantly influence the adsorption process of MO dye. For example, Hydroxyl groups can form hydrogen bonds with the nitro ($–NO_2$) and sulfonate ($–SO_3^-$) groups of the MO molecule. Carbonyl groups can act as electron acceptors and interact with the electrophilic groups present in methyl orange. These groups may form stable double bonds with the dye, enhancing the stability of the adsorption process and positively influencing the adsorption capacity. Furthermore, benzene rings can interact with MO through van der Waals forces and π-π stacking interactions. These interactions may enhance the adsorption capacity of the adsorbent.

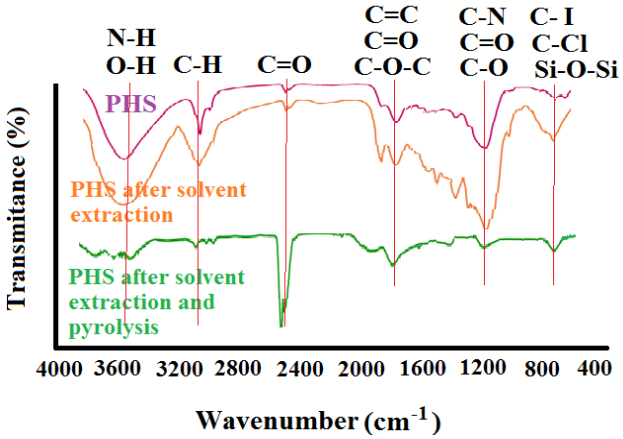

Figure 2. FTIR spectra of the produced biosorbents by various activation methods.

3.3. XRD analysis

XRD patterns of the pyrolyzed PHS and pyrolyzed PHS after phosphoric acid chemical activation are reported in **Figure 3**. As depicted in this figure, the broad band at about 24° and 43° with no any sharp peak show the presence of carbon amorphous phase in the produced biosorbents [27, 28]. However, for chemical activated sample, a relatively sharp peak at about 33° can reveal the presence of phosphorus atoms in the sample structure.

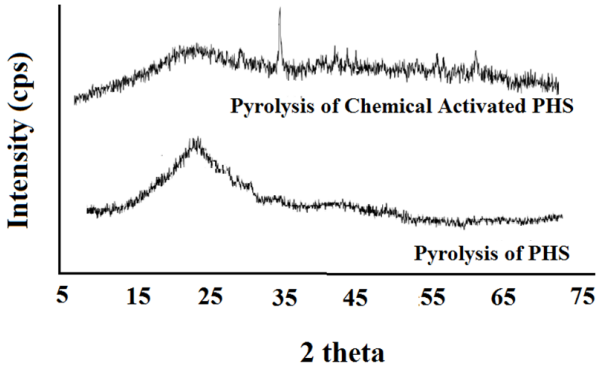

Figure 3. XRD patterns of the produced biosorbents with and without chemical activation.

3.4. The effects of activation method on the adsorption capacity of methyl orange

Activation of the produced biosorbents is very important process. Because, during the activation process the specific surface of particles increased as well as increasing the adsorption capacity of biosorbents [29]. Solvent extraction, chemical activation with phosphoric acid, and the pyrolysis are different methods, which were used in this work for activation of the produced biosorbents. The adsorption capacity of produced biosorbents by using different activation methods were reported in **Figure 4.** Because of very low-capacity values (in comparison to others), and introducing some painting and oily components into the system, the adsorption capacity of raw sawdust is not reported here. For all the studied dye concentrations, the adsorption capacity of PHS after the solvent extraction process is below 90 mg/g. After chemical activation with phosphoric acid, the adsorption sites on the surface of sample increased and therefore the adsorption capacity of the PHS particles increased several times and reached to about 600 mg/g in higher dye concentrations. Finally, the adsorption capacity of PHS sample reaching its maximum value of about 720 mg/g after the pyrolysis process.

Solvent extraction process led to extract the relatively all extractable components, such as essential oils, lipids, and so on. Therefore, the empty sites were performed on the surface of particles after drying and they may increase the adsorption surface of samples. Phosphoric acid chemical activation modifies the textural properties and surface characteristics of the biosorbent, resulting in a higher adsorption capacity [30]. Phosphoric acid acts as a dehydrating agent, promoting the formation of porous structures. It helps in creating a network of micropores and mesopores, which increases the surface area of the produced biosorbent. Chemical activation can introduce or modify various functional groups on the carbon surface, such as hydroxyl (-OH), carbonyl (C=O), and phosphate groups (PO_4). These groups can enhance the adsorption capacity by providing additional active sites for interaction with adsorbates. Finally, as mentioned in the literature [31, 32], the pyrolysis process under a neutral atmosphere leads to higher specific surfaces and the higher adsorption capacities were achieved. Therefore, the highest adsorption capacity of biosorbent is shown after the pyrolysis process.

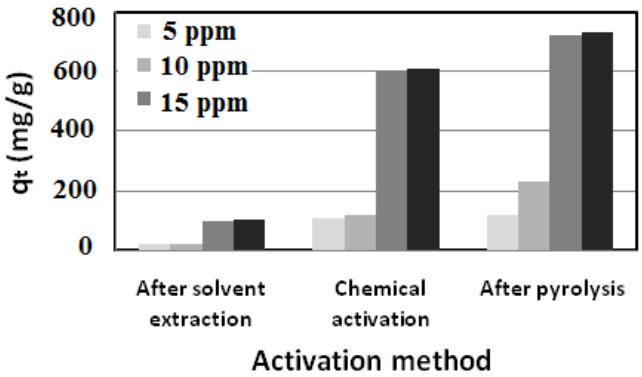

Figure 4. The adsorption capacities of the different produced biosorbents from different activation methods.

3.5. The effects of dose of biosorbent on the adsorption capacity of methyl orange

The adsorption capacities of biosorbents for the adsorption of MO dye contaminant, at a solution concentration of 20 ppm, were reported in **Figure 5** in various doses of the used adsorbent. As can be seen, except for the biosorbent after chemical activation and at 0.01 g dose of biosorbent, by increasing the biosorbent dosage from 0.01 g to 0.1 g in the 100 ml of stoke solution the adsorption capacity of the biosorbent decreased continuously. For example, for the pyrolyzed biosorbent by increasing the dose of biosorbent the adsorption capacity decreased from 1350 to 160 mg/g. However, at biosorbent dosages greater than 0.05 g, the adsorption capacity remained relatively constant. At higher dosages of biosorbent, oversaturation or coverage of active sites occurs and it causes to reduce the availability of binding sites for dye contaminants. Relatively, similar results have been reported in the literature for the adsorption of ciprofloxacin and methylene blue [33, 34].

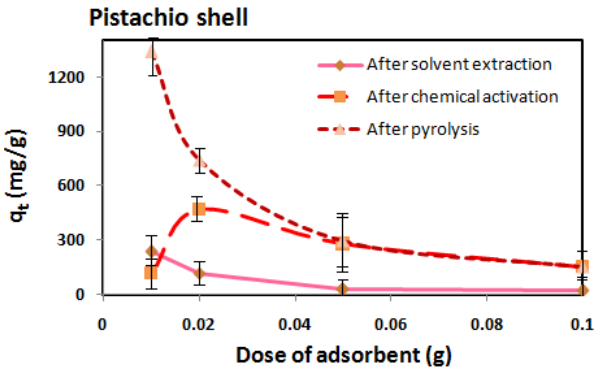

Figure 5. The adsorption capacities of the biosorbents in the various doses of samples.

3.6. The effects of solution concentration on the adsorption capacity of methyl orange

The effect of the initial concentration of the dye component on the adsorption capacity of the various produced biosorbents is illustrated in **Figure 6**. In this figure, the solution concentration ranges from 5 to 50 ppm, with a constant biosorbent dose of 0.2 g/L at neutral pH. As the concentration of the dye component increased from 5 to 15 ppm, the adsorption capacity of the produced biosorbents increased significantly. However, at solution concentrations exceeding 15 ppm, no substantial increase in adsorption capacities was observed. This phenomenon occurs because, as the initial dye concentration rises, the driving force for mass transfer increases, promoting the biosorption of methyl orange (MO). However, beyond an initial concentration of 15 ppm, the saturation of active sites on the surface of the biosorbent takes place, leading to stabilization in the amount of dye removed [35, 36].

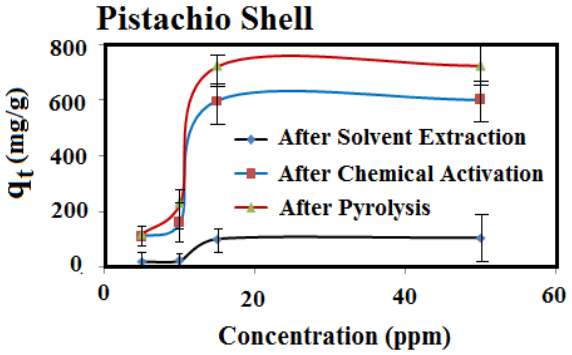

Figure 6. The adsorption capacities of the produced biosorbents in the various concentrations of solution.

3.7. Adsorption isotherm

The adsorption mechanisms, adsorbent–adsorbate interactions, surface properties, and adsorption capacity of the produced biosorbents were investigated using isotherm studies based on three models: Langmuir, Freundlich, and Sips. The details of the studied kinetic models are provided in the literature [21]. **Table 1** summarizes the estimated

constants and statistical parameters obtained from these three selected isotherm models. The comparison of the reported R^2 values reveals a strong agreement between the calculated values and the experimental results, with R^2 values exceeding 0.95. However, among all the studied samples, the Sips isotherm model, which includes three adjustable parameters, demonstrates the best fit to the experimental data ($R^2 > 0.99$). The Sips isotherm model combines the key characteristics of both the Freundlich and Langmuir isotherms, making it suitable for scenarios where both neighboring interactions and heterogeneous adsorption are present. A comparison between the Freundlich and Langmuir isotherm models indicates that the Langmuir model provides a better fit for the experimental data, as evidenced by R^2 values closer to one. Therefore, the monolayer adsorption model governs the adsorption of methyl orange dye molecules on the surfaces of biosorbents produced from pistachio hard skin (PHS) using three different activation methods. For the Sips model, values of *m* less than 1 indicate that physical adsorption predominates over chemical adsorption. Additionally, values around 0.13 for this parameter suggest heterogeneity in the adsorption sites, indicating that adsorption occurs in a nonlinear manner with a gradual increase in slope.

Table 1. The isotherm parameters for the different used models.

	After solvent extraction				After chemical activation				After pyrolysis			
	K	**N_O**	**m**	**R^2**	**K**	**N_O**	**m**	**R^2**	**K**	**N_O**	**m**	**R^2**
Langmuir	0.045	158.9	-	0.98	0.05	892.9		0.98	0.05	1089.0	-	0.98
Freundlich	14.18	-	1.89	0.98	90.90	-	1.98	0.97	108.8	-	1.97	0.97
Sips	2.0×10^{-8}	105.3	0.13	0.99	1.3×10^{-8}	608.7	0.13	0.99	3.2×10^{-8}	738.4	0.14	0.99

4. Conclusions

The production of biosorbents from the hard skin of pistachios (Pistachios Hub) and the effects of various activation methods on the adsorption capacity of the resulting biosorbents were investigated. This study utilized three activation methods: solvent extraction, chemical activation with phosphoric acid, and pyrolysis. According to the reported results, the produced biosorbents demonstrated a significant ability to absorb methyl orange (MO) from contaminated water. The adsorption capacity of the samples increased significantly following chemical activation; however, the maximum adsorption capacity was achieved after the pyrolysis process. Additionally, a biosorbent dosage of 0.01 g in 100 ml of stock solution was found to be the optimal amount, yielding the highest adsorption capacity. Based on the reported results, the synthesized biosorbents, particularly those produced through the pyrolysis process; demonstrate good potential for the adsorption of MO. A comparison between the produced biosorbents from the PHS precursor was reported in **Table 2**. However, the conditions in real wastewater are much more complex. This is primarily due to the presence of a wide range of chemicals with vastly different properties. Various types of cationic, anionic, and azo dyes, along with auxiliary substances used in processes such as soaps, oils, and residual surfactants like emulsifiers, are present in actual wastewater, significantly affecting each other's adsorption capabilities. Although this study did not conduct adsorption processes on real wastewater, it is recommended that future work utilize the synthesized adsorbents for the removal of pollutants from real wastewater.

Table 2. Comparison between the produced biosorbents from the PHS precursor.

Precursor	Adsorbed contaminant	Activation method	q_{max} (mg/g)	Ref.
PHS	Nickel (II)	Chemical activation	19.37	[37]
PHS	Nitrate	Pyrolysis	211.6	[38]
PHS	Methylene Blue	Chemical Activation with $ZnCl_2$,	321	[39]
	Iodine	Pyrolysis	1276	
PHS	Toluene	Alkylation & Pyrolysis	169.9	[40]
	Ethyl Acetate		96.7	
PHS	Methyl Paraben	Pyrolysis	55.5	[41]
PHS	Methyl Orange	Solvent Extraction, Chemical Activation, Pyrolysis	1350	This work

Authors' contributions

Hadi Baseri: Writing –original draft, Visualization, and Project administration. **Pooya Fazlali,** and **Amir Hussein Hooshmand Poor:** Methodology and Investigation.

Declaration of competing interest

The authors declare that they have no known competing financial interests or personal relationships that could have appeared to influence the work reported in this paper.

Funding

This paper received no funding.

Data availability

Data will be made available on request.

References

[1] S. Nag, J. Das, S. Biswas, B.K. Lodh, Experimental and ANN based process optimization for bioremediation of Cr^{6+} and Cd^{2+} by green adsorbent prepared from artocarpus heterophyllus leaves, J. Indian Chem. Soc. 102 (2025) 101485.
DOI: https://doi.org/10.1016/j.jics.2024.101485

[2] P. Parthasarathy, T. Al-Ansari, H.R. Mackey, K.S. Narayanan, G. McKay, A review on prominent animal and municipal wastes as potential feedstocks for solar pyrolysis for biochar production, Fuel 316 (2022) 123378.
DOI: https://doi.org/10.1016/j.fuel.2022.123378

[3] I.M. Toplicean, A.D. Datcu, An overview on bioeconomy in agricultural sector, biomass production, recycling methods, and circular economy considerations, Agriculture, 14(7) (2024) 1143.
DOI: https://doi.org/10.3390/agriculture14071143

[4] A. Lakhouit, W.S. Al Rashed, S.Y.H. Abbas, M. Shaban, Integrating machine learning for precision agriculture waste estimation and sustainability enhancement, Comput. Electron. Agric. 230 (2025) 109933.
DOI: https://doi.org/10.1016/j.compag.2024.109933

[5] Y. Wibisono, E.T. Anggraeni, D. Alvianto, S.R. Ummah, D.H.Y. Yanto, T.A. Kurniawan, H.A. Tajarudin, W.A. Nugroho, Valorization of agricultural waste through microbial fermentation into industrial-grade bio-succinic acid: A review, Biomass Bioenergy 202 (2025) 108183.
DOI: https://doi.org/10.1016/j.biombioe.2024.108183

[6] M. Mohammadi, I. Harjunkoski, Circular supply chains for sustainable use of biomass, Comput. Chem. Eng. 204 (2026) 109368.
DOI: https://doi.org/10.1016/j.compchemeng.2024.109368

[7] A.M. Tubeileh, G.T. Stephenson, Soil amendment by composted plant wastes reduces the Verticillium dahliae abundance and changes soil chemical properties in a bell pepper cropping system, Curr. Plant Biol. 22 (2020) 100148.
DOI: https://doi.org/10.1016/j.cpb.2020.100148

[8] H. Kowalska, K. Czajkowska, J. Cichowska, A. Lenart, What's new in biopotential of fruit and vegetable by-products applied in the food processing industry, Trends Food Sci. Technol. 67 (2017) 150-159.
DOI: https://doi.org/10.1016/j.tifs.2017.06.018

[9] A. Kashtiaray, P. Ghorbani, Z. Rashvandi, M.M. Salehi, A. Mohammadi, F. Rasouli Asl, F. Ganjali, S. Sadeghmarand, A. Maleki, A cleansing magnetic nanosystem made of Fe/Zn/MIL101-embedded Arabic Gum rich of chlorophyllin: Photodegradation of Eriochrome black-T and pathogens in water media, Colloids Surf. A Physicochem. Eng. Asp. 709 (2025) 136121.
DOI: https://doi.org/10.1016/j.colsurfa.2024.136121

[10] M.M. Salehi, M. Mohammadi, A. Maleki, E.N. Zare, Performance of magnetic nanocomposite based on xanthan gum-grafted-poly(acrylamide) crosslinked by borax for the effective elimination of amoxicillin from aquatic environments, Chemosphere 361 (2024) 142548.
DOI: https://doi.org/10.1016/j.chemosphere.2024.142548

[11] M.M. Salehi, S.M. Nezhad, L. Choopani, S. Asghari, S.M. Safavi, F. Shirini, H. Gholamikafshgari, A. Maleki, E.N. Zare, Magnetic carrageenan gum-grafted-polyacrylamide nanocomposite for uptake of cationic dyes from the aquatic systems, Int. J. Biol. Macromol. 283 (2024) 137796.
DOI: https://doi.org/10.1016/j.ijbiomac.2024.137796

[12] J. Rahimi, M.T. Ijdani, H. Abbasi, M.M. Salehi, A. Maleki, Two-dimensional imide-based covalent organic frameworks for cationic dye adsorption: Synthesis, characterization, isotherm, kinetics, and thermodynamic analysis, J. Hazard. Mater. Adv. 18 (2025) 100680.
DOI: https://doi.org/10.1016/j.hazadv.2024.100680

[13] F. Zahaf, M.A. Bekhti, O. Saiah, R. Marouf, J. Schott, Dynamic biosorption of Basic Fuchsin by Pinus brutia cones: A comparison of the effects of different pretreatment conditions analysis of kinetics and thermodynamics, Desalination Water Treat. 324 (2025) 101422.
DOI: https://doi.org/10.1016/j.dwt.2025.101422
[14] S.R. Yasin, S.S. Jasim, I.A. Al-Baldawi, Removal of lead, cadmium, and copper from wastewater using Cinnamon bark waste to introduce it as a value-added product: Removal, kinetics and thermodynamics study, Desalination Water Treat. 323 (2025) 101345.
DOI: https://doi.org/10.1016/j.dwt.2025.101345
[15] S. Sundararaman, S. Dhanasekaran, A.S. Vickram, J.A. Kumar, M.Y. Priya, Sahana, M.R. Soosai, A. Santhanakrishnan, P. Jangir, M. Khishe, G. Gulothungan, Strategic engineering and functional mechanism elucidation of advanced materials in detoxification of contaminated water matrices, Results Eng. 26 (2025) 104851.
DOI: https://doi.org/10.1016/j.rineng.2024.104851
[16] S. Kainth, P. Sharma, O.P. Pandey, Green sorbents from agricultural wastes: A review of sustainable adsorption materials, Appl. Surf. Sci. Adv. 19 (2024) 100562.
DOI: https://doi.org/10.1016/j.apsadv.2024.100562
[17] K.G.N. Quiton, S.P.V. Baltazar, T.B. Nguyen, C.W. Chen, C.D. Dong, Advances in modified and unmodified rice straw-based biosorbents for water and wastewater treatment: Current progress and future perspectives, Sep. Purif. Technol. 378(1) (2025) 134473.
DOI: https://doi.org/10.1016/j.seppur.2024.134473
[18] H. Baseri, A. Farhadi, Catalytic Pyrolysis of Pistachio Shell for the Production of Different Biosorbents for Adsorption of Various Contaminants from the Contaminated Water, Int. J. Environ. Res. 19 (2025) 110.
DOI: https://doi.org/10.1007/s41742-025-00648-3
[19] I. Neme, G. Gonfa, C. Masi, Activated carbon from biomass precursors using phosphoric acid: A review, Heliyon 8(12) (2022) e11940.
DOI: https://doi.org/10.1016/j.heliyon.2022.e11940
[20] H. Megherbi, H. Runtti, S. Tuomikoski, A. Heponiemi, T. Hu, U. Lassi, A. Reffas, The effect of phosphoric acid on the properties of activated carbons made from Myrtus communis leaves: Textural characteristics, surface chemistry, and capacity to adsorb methyl orange, J. Mol. Struct. 1321 (2025) 140038.
DOI: https://doi.org/10.1016/j.molstruc.2024.140038
[21] L. Choopani, M.M. Salehi, H. Mashhadimoslem, M.S. Khosrowshahi, M. Rezakazemi, A.A. AlHammadi, A. Elkamel, A. Maleki, Removal of organic contamination from wastewater using granular activated carbon modified—Polyethylene glycol: Characterization, kinetics and isotherm study, PLOS ONE 19 (2024) e0304684.
DOI: https://doi.org/10.1371/journal.pone.0304684
[22] A.W. Suciyati, P. Manurung, S. Sembiring, R. Situmeang, Comparative study of Cladophora sp. cellulose by using FTIR and XRD, J. Phys. Conf. Ser. 1751 (2021) 012075.
DOI: https://doi.org/10.1088/1742-6596/1751/1/012075
[23] S. Cichosz, A. Masek, K. Dems-Rudnicka, Original study on mathematical models for analysis of cellulose water content from absorbance/wavenumber shifts in ATR FT-IR spectrum, Sci. Rep. 12 (2022) 19739.
DOI: https://doi.org/10.1038/s41598-022-24158-w
[24] V. Hospodarova, E. Singovszka, N. Stevulova, Characterization of Cellulosic Fibers by FTIR Spectroscopy for Their Further Implementation to Building Materials, Am. J. Anal. Chem. 9 (2018) 303.
DOI: https://doi.org/10.4236/ajac.2018.95023
[25] R. Javier-Astete, J. Jimenez-Davalos, G. Zolla, Determination of hemicellulose, cellulose, holocellulose and lignin content using FTIR in Calycophyllum spruceanum (Benth.), PLoS ONE 16 (2021) e0256559.
DOI: https://doi.org/10.1371/journal.pone.0256559
[26] G. Ezequiel, Fourier transform infrared spectroscopy in treated woods deteriorated by a white rot fungus, Maderas Cienc. Tecnol. 20 (2018) 479.
DOI: https://doi.org/10.4067/S0718-221X2018005004701
[27] Y.S. Reddy, A. Naveed, H. Wang, K. Rambabu, M. Sivaraju, F. Banat, Sustainable mesoporous graphitic activated carbon as biosorbent for efficient adsorption of acidic and basic dyes from wastewater: Equilibrium, kinetics and thermodynamic studies, J. Hazard. Mater. Adv. 9 (2023) 100214.
DOI: https://doi.org/10.1016/j.hazadv.2022.100214
[28] J.A. Nisha, J. Janaki, V. Sridharan, G. Padma, M. Premila, T.S. Radhakrishnan, X-ray diffraction and thermoanalytical investigations of amorphous carbons derived from C60, Thermochim. Acta 286(1) (1996) 17-24.
DOI: https://doi.org/10.1016/0040-6031(96)02928-4
[29] J.L.S. Duarte, A. Hayat, C.M. Domínguez, A. Santos, S. Cotillas, Forest biomass derived biochar for effective meropenem mitigation in hospital effluents, J. Hazard. Mater. Adv. 19 (2025) 100811.
DOI: https://doi.org/10.1016/j.hazadv.2024.100811
[30] W.A. Khanday, M.J. Ahmed, P.U. Okoye, E.H. Hummadi, Single-step H3PO4 activation of chitosan for efficient adsorption of amoxicillin and doxycycline antibiotic pollutants, Inorg. Chem. Commun. 175 (2025) 114189.
DOI: https://doi.org/10.1016/j.inoche.2025.114189

[31] S. Paşa, N. Yılmaz, İ. Bulduk, O. Alagöz, Effective adsorption performance of hemp root-derived activated carbon for tamoxifen-contaminated wastewater, J. Mol. Liq. 425 (2025) 127219.
DOI: https://doi.org/10.1016/j.molliq.2024.127219
[32] S. Mishra, M.K. Adsorptive removal of diclofenac on nanoporous anoxic sewage sludge biochar: Investigating the influence of carbonization temperature, Sep. Purif. Technol. 354 (2025) 129322.
DOI: https://doi.org/10.1016/j.seppur.2024.129322
[33] Y. Gherraby, Y. Rachdi, M. El Alouani, B. Aouan, R. Bassam, R. Cherouaki, H. Saufi, E.H. Khouya, S. Belaaouad, Application of Aptenia cordifolia powder as a biosorbent for methylene blue retention from an aqueous medium: Isotherm, kinetic, and thermodynamic investigations, Desalination Water Treat. 318 (2024) 100263.
DOI: https://doi.org/10.1016/j.dwt.2024.100263
[34] E.B. Vamsi, M. Reshma, C.P. Devatha, Adsorption of ciprofloxacin antibiotic using chitosan graphene oxide hybrid beads, Case Stud. Chem. Environ. Eng. 10 (2024) 100982.
DOI: https://doi.org/10.1016/j.cscee.2024.100982
[35] A.H. Jawad, A.S. Abdulhameed, Mesoporous Iraqi red kaolin clay as an efficient adsorbent for methylene blue dye: adsorption kinetic, isotherm and mechanism study, Surf. Interfaces 18 (2020) 100422.
DOI: https://doi.org/10.1016/j.surfin.2020.100422
[36] S. Rahmani, B. Zeynizadeh, S. Karami, Removal of cationic methylene blue dye using magnetic and anionic-cationic modified montmorillonite: kinetic, isotherm and thermodynamic studies, Appl. Clay Sci. 184 (2020) 105391.
DOI: https://doi.org/10.1016/j.clay.2019.105391
[37] M.H. Salmani, M.T. Ghaneian, M.H. Ehrampoush, M.H. Rezaeizadeh, Evaluation of adsorption efficiency of raw and modified pistachio hard skin in removal of Ni(II) from the contaminated solution, Desalination Water Treat. 153 (2019) 157-164.
DOI: https://doi.org/10.5004/dwt.2019.23982
[38] R. Akbarpour, Z. Hajebrahimi, M. Dolatabadi, Removing nitrate from contaminated water using activated carbon prepared from hard pistachio shells, Pistachio Health J. 4(2) (2021) 28-39.
DOI: https://civilica.com/doc/1275004
[39] O. Baytar, Ö. Şahin, C. Saka, S. Ağrak, Characterization of microwave and conventional heating on the pyrolysis of pistachio shells for the adsorption of methylene blue and iodine, Anal. Lett. 51(14) (2018) 2205-2220.
DOI: https://doi.org/10.1080/00032719.2017.1415918
[40] T. Cheng, J. Li, X. Ma, L. Zhou, H. Wu, L. Yang, Alkylation modified pistachio shell-based biochar to promote the adsorption of VOCs in high humidity environment, Environ. Pollut. 295 (2022) 118714.
DOI: https://doi.org/10.1016/j.envpol.2021.118714
[41] H.R. Nodeh, H. Sereshti, S. Ataolahi, A. Toloutehrani, A.T. Ramezani, Activated carbon derived from pistachio hull biomass for the effective removal of parabens from aqueous solutions: isotherms, kinetics, and free energy studies, Desalination Water Treat. 201 (2020) 155-164.
DOI: https://doi.org/10.5004/dwt.2020.25995